



High sensitivity profiling of *N*-glycans from mouse serum using fluorescent imidazolium tags by HILIC electrospray ionisation spectrometry

Yao-Yao Zhang^{a,b,c}, Si-Yu Zhang^a, Zi-Xuan Hu^a, Josef Voglmeir^a, Li Liu^{a,*}, M. Carmen Galan^{c,*}, Mattia Ghirardello^{c,d,*}

^a Glycomics and Glycan Bioengineering Research Center (GGBRC), College of Food Science and Technology, Nanjing Agricultural University, 1 Weigang, 210095 Nanjing, China

^b Lipid Technology and Engineering, School of Food Science and Engineering, Henan University of Technology, Lianhua Road 100, 450001 Zhengzhou, China

^c School of Chemistry, University of Bristol, Cantock's Close, BS8 1TS Bristol, UK

^d Department of Chemistry, Instituto de Investigación en Química de la Universidad de La Rioja (IQUR), Universidad de La Rioja, 26006 Logroño, La Rioja, Spain

ARTICLE INFO

Keywords:

Mouse serum glycans
Glycan labeling
Imidazolium tags
MS detection
Fluorescence detection
Glycoproteins

ABSTRACT

N-linked glycosylation is a ubiquitous protein post-translational modification in which aberrant glycan biosynthesis has been linked to severe conditions like cancer. Accurate qualitative and quantitative analysis of *N*-glycans are crucial for investigating their physiological functions. Owing to the intrinsic absence of chromophores and high polarity of the glycans, current detection methods are restricted to liquid chromatography and mass spectrometry. Herein, we describe three new imidazolium-based glycan tags: 2'GITag, 3'GITag, and 4'GITag, that significantly improve both the limit of detection and limit of quantification of derivatized oligosaccharides, in terms of fluorescence intensity and ionisation efficiency. Our top-performing derivatisation agent, 4'GITag, shifted the detection sensitivity range from high femtomole to sub-femtomole levels in ESI-MS compared to traditional glycan label, 2AB, enabling the identification of 24 *N*-glycans in mouse serum, including those bearing sialic acids. Additionally, 4'GITag stabilized Na-salt forms of sialic acids, simplifying the simultaneous analysis of neutral and negative charged *N*-glycans significantly, avoiding the need for complex derivatisation procedures typically required for the detection of sialylated species. Overall, the favorable performance of imidazolium tags in the derivatisation and sensitive profiling of glycans has the potential for labeling tissue or live cells to explore disease biomarkers and for developing new targeted therapeutic strategies.

1. Introduction

Glycosylation represents one of the most abundant and complex protein post-translational modifications that greatly amplifies the protein structural features and functions and plays fundamental roles in virtually any biological process (Schjoldager et al., 2020; Varki, 2017). For instance, changes in the glycome are observed features of many critical human conditions such as cardiovascular diseases, neurological disorders, microbial infections, and are key modulators in cancer onset and development (Kizuka et al., 2017; Magalhães et al., 2017; Wright et al., 2017; Zilmer et al., 2020). Alterations in glycan biosynthesis lead to significant modifications in the branching pattern, elongation, and degree of fucosylation and sialylation of *N*-glycans, thereby reflecting a person's health or disease status through their cellular glycoprofile (Mereiter et al., 2019; Reily et al., 2019). The development of sensitive

glycomics techniques allowed deciphering the glycode associated with diseases, delivering new glycan-based biomarkers to enable a timely diagnosis and more effective therapeutic approaches. For instance, sialyl-Lewis A (also known as Cancer Antigen 19-9, or CA 19-9, Lewis A bears an antigen expressed on red blood cells and other epithelial surfaces) is the most well-validated serological biomarker for pancreatic cancer detection (Luo et al., 2021). Similarly, CA-125 is a glycopeptide epitope of MUC16 and is the only clinically relevant biomarker for ovarian cancer detection (Malaker et al., 2022). Moreover, several sialylated glycans, such as A3G3S3, have recently been identified as relevant biomarkers for predicting HIV remission following antiretroviral therapy (Giron et al., 2021). Unfortunately, the immense structural diversity of glycans, given by differences in glycoside composition, anomeric configurations, branching positions, and site-specific functionalizations, presents a formidable challenge for glycan

* Corresponding authors.

E-mail addresses: lichen.liu@njau.edu.cn (L. Liu), m.c.galan@bristol.ac.uk (M.C. Galan), mattia.ghirardello@unirioja.es (M. Ghirardello).

<https://doi.org/10.1016/j.carbpol.2024.122449>

Received 27 March 2024; Received in revised form 21 June 2024; Accepted 27 June 2024

Available online 30 June 2024

0144-8617/© 2024 The Authors. Published by Elsevier Ltd. This is an open access article under the CC BY license (<http://creativecommons.org/licenses/by/4.0/>).

analysis (Sethi et al., 2016).

The primary analytical techniques for investigating the complex structural details of glycans encompass mass spectrometry (MS) coupled with liquid chromatography (LC-MS), including electrospray ionisation (ESI) (Wagt et al., 2022), and matrix-assisted laser desorption/ionisation (MALDI) (Ressom et al., 2008; Zhu et al., 2015), as an ionisation method, orbitrap (Cho et al., 2022) and triple quadrupole (Alvarez et al., 2022) as analysers, and collision-induced/activated dissociation (CID/CAD), or electron-transfer dissociation (ETD) (Alagesan et al., 2019) as dissociation methods. Ion-mobility (IM) spectrometry has proven to be a potent tool for the unambiguous identification of glycans or their MS/MS derived ionic fragments (Bechtella et al., 2024; Manz et al., 2022; Pallister et al., 2020; Vos et al., 2023). Moreover, Tandem mass spectrometry (MS/MS) also showed to provide quantitative and structural information for the identification of glycans from complex matrices (Li et al., 2023).

Additionally, the application of orthogonal characterisation techniques such as nuclear magnetic resonance (NMR) (Quintana et al., 2023; Sasaki et al., 2014) and chromatographic approaches for analyte separation, such as liquid chromatography (LC) (Bones et al., 2010; Liu et al., 2023) and capillary electrophoresis (CE) (Zhou et al., 2022), play crucial roles in glycan analysis.

Unfortunately, a major challenge in glycan analysis is the limited amount of protonation sites, available on glycan structures. These protonation sites, typically nitrogenated functional groups, are necessary for the derivatization of glycan structures into charged species for an efficient and sensitive MS detection.

To address this issue, glycan derivatisation strategies with fluorescent or hydrophobic probes have provided a valuable tool for their separation through LC and detection through UV/VIS or ESI-MS techniques (Cai et al., 2014; Cai et al., 2017). 2-Aminobenzamide (2-AB, compound 1 in Fig. 1) is considered the gold standard for *N*-glycan derivatisation, offering good *N*-glycan detection performance by providing stable and reproducible fluorescence labelling of glycans in LC (Melo et al., 2022; Zhang et al., 2022). However, previous studies have demonstrated that 2AB derivatisation fails to increase the ionisation efficiency in comparison to underivatized glycans within MS applications, positioning it as a less optimal derivatisation agent for both qualitative and quantitative MS analysis of glycans (Keser et al., 2018). To enhance the ionisation efficiency of glycan analysis in MS, procainamide (Pro A) and RapiFluor-MS (RF-MS) fluorescent tags were developed which demonstrated improved detection efficiency of IgG *N*-glycans regarding fluorescence and ionisation efficiency compared to 2AB (Keser et al., 2018). Although RapiFluor-MS exhibited fast and throughput *N*-glycomics profiling, Pro A and RF-MS showed comparable

limits of quantification with both fluorescence and MS detection (Messina et al., 2021). Additionally, the high cost of RF-MS and the complexity of sample processing are also essential factors that need to be taken into consideration. To further enhance the performance of glycan detection sensitivity in MS, novel glycan labels with permanent positive charges, such as the Girard's reagent T (GT) and P (GP) (Le et al., 2018) and their derivatives (Kianfar, 2020; Mahmoudi et al., 2019), have been developed to improve ionisation efficiency. However, the use of Girard's hydrazine-based labelling method faces challenges, including reversibility and the requirement for harsh acidic conditions during the labelling process, which often leads to retro-hydrazone formation and consequently the decrease in detection sensitivity (Ghirardello et al., 2022). This is particularly crucial for labile glycosides, such as sialylated residues, which often undergo cleavage reactions during the labelling process and MALDI MS analysis (Aich et al., 2014; Marie et al., 2023; Shao et al., 2003; Zhang et al., 2019). Moreover, to boost the glycan detection through the application of more efficient and sensitive tags, the use of MS probes containing a *N*-methylimidazolium moiety, which carries a permanent positive charge, has been shown to boost the detection of glycans, especially when the analytes are present in trace amounts (Benito-Alifonso et al., 2016; Sittel & Galan, 2015). We previously adapted this strategy to develop an arylamine imidazolium Tag (GITag, compound 2 in Fig. 1), which outperformed 2AB in terms of glycan limit of detection (LOD) and limit of quantification (LOQ) in ESI-MS analysis (Zhang et al., 2021). Remarkably, the GITag labelling procedure allows the direct derivatisation of *N*-glycans released from human serum on the MALDI MS target plate, streamlining the identification of sialylated glycans. However, the GITag's use of a labile ester linkage between the imidazolium MS reporter and the arylamine moiety risks undesired hydrolysis reactions during the labelling procedure and MALDI MS analysis. This could lead to an underestimation of the actual glycan content, highlighting a limitation to the GITag's labelling efficiency.

To enhance glycan detection sensitivity in complex matrices like sera through imidazolium tags, we have now developed a second generation of GITags with improved chemical stability and MS detection sensitivity in addition to an improved fluorescence emission profile, suitable for biomedical applications. Herein, we provide a robust synthetic approach for the preparation of novel GITag labels, namely, 2'GITag, 3'GITag, and 4'GITag (compounds 3–5, Fig. 1) and demonstrate their superior glycan detection sensitivity.

Initial efforts were devoted to improving the efficiency of the GITag reporters. To that end, we decided to replace the ester linkage connecting the arylamine and the imidazolium moiety with a more stable amide motif. This change also resulted in improved overall synthetic yields for the GITags. Furthermore, to evaluate how structural and electronic alterations in the aromatic scaffolds influence the fluorescence and glycan labelling efficiency of the different GITags, we generated *ortho*-, *meta*- and *para*- substituted GITags and tested them on mono- and disaccharide model systems. Additionally, the glycan derivatisation conditions were optimised using *N*-glycans released from the horseradish peroxidase (HRP), which served as a standard glycoprotein, while the effectiveness of the GITag labelling method for identifying *N*-glycans was tested in mouse serum glycoproteins. These glycans were labelled and profiled using the newly developed 2'GITag (3), 3'GITag (4) and 4'GITag (5) analogues. In this work, we synthesized GITags (3–5) featuring an arylamine unit and an imidazolium MS reporter. The tags are designed to chemoselectively undergo activation under acidic conditions, facilitating their conjunction with released glycans through reductive amination. We hypothesize that this innovation, particularly with 4'GITag (5), not only enhances glycan detection to femtomolar levels but also significantly broadens the detectable spectrum of sialoglycans beyond the capabilities of the conventional 2AB approach. Our results suggest a substantial leap in glycomics analysis, potentially enabling more sensitive detection of disease-associated glycans.

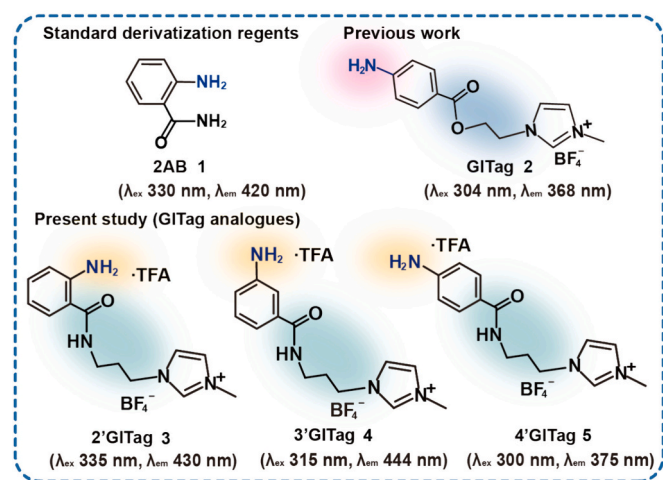


Fig. 1. Structures of different glycan derivatisation reagents: 2AB (1), GITag (2), 2'GITag (3), 3'GITag (4), and 4'GITag (5).

2. Materials and methods

2.1. Materials

3-Bromopropylamine hydrobromide, 2-aminobenzamide (2AB), 4-aminobenzoic acid, 3-aminobenzoic acid, di-tert-butyl dicarbonate, *N*-methylimidazolium, potassium tetrafluoroborate (KBF₄), *N*-hydroxy succinimide (NHS), *N,N*-diisopropylethylamine (DIPEA) and dicyclohexylcarbodiimide (DCC) were purchased from J&G chemicals (Nanjing, China); Sodium cyanoborohydride (NaBH₃CN), *N*-acetyl-D-glucosamine (GlcNAc) and Lactose monohydrate were supplied by Aladdin Chemicals Co. (Shanghai, China); Dichloromethane (CH₂Cl₂), ethyl acetate (EtOAc), methanol (MeOH), acetonitrile (ACN), were obtained from General-Reagent Co. (Shanghai, China); Acetonitrile (ACN) used for HPLC analysis was purchased from Merck. (Nanjing, China). Mouse serum was obtained from Yuanye Bio-Technology Co., Ltd. (Shanghai, China); Other bulk chemicals were obtained from commercial suppliers without further purification or modification.

2.2. Imidazolium tag preparation and characterisation

The preparative-scale syntheses of 4'GITag (5), 2'GITag (3), and 3'GITag (4) were performed as described in the ESI section 1. NMR spectra were recorded on 400/300 MHz NMR at 298 K. Chromatographic analyses were performed using a Nexera UPLC-FLD system coupled to an LCMS 8040 ESI mass spectrometer (both from Shimadzu Company, Kyoto, Japan). High resolution Electrospray ionisation (ESI) mass spectra were recorded on a Micromass LCT mass spectrometer or a VG Quattro mass spectrometer.

2.3. *N*-glycan extraction

The method of enzymatic *N*-glycan release using PNGase used a previously developed and standardized protocol, optimised and described in the literature (Du et al., 2018; Guo et al., 2020) as referenced in ESI section 1.2.

N-glycan release from HRP glycoprotein was performed according to a previously reported procedure (Du et al., 2018). Aliquots of HRP glycoprotein (2 µL) were mixed with water (16 µL) and denatured at 95 °C for 10 min. After cooling the solution to room temperature, phosphate-citrate buffer (12 µL, pH 2.0) and PNGase Rc (10 µL, 1.8 µg/µL) were added into the heat-denatured sample and incubated at 37 °C for 16 h.

The release of *N*-glycans from mouse serum glycoproteins was conducted following previously established procedures (Guo et al., 2020). An aliquot of 50 µL mouse serum was mixed with 90 µL of water and subjected to denaturation at 95 °C for 10 min. After cooling to room temperature, 60 µL of phosphate buffer (500 mM, pH 7.5), 100 µL of urea (6 M), 25 µL of SDS β-mercaptoethanol (2 % v/v), and 40 µL of Triton X-100 (10 % w/v) was added. Afterwards, 200 µL of PNGase F was added, and the mixture was incubated at 37 °C for 16 h. The subsequent purification of the *N*-glycans from both the HRP and mouse serum glycoproteins utilised pre-packed porous graphite solid-phase extraction (SPE) carbon columns (for more details see ESI section 1).

2.4. Model oligosaccharides derivatization and purification

The labelling of oligosaccharides was performed following previously reported procedures with minor modifications, using MeOH/acetic acid (7/3, v/v) as the solvent mixture and incubating at 65 °C for 2 h (Zhang et al., 2019). The obtained mono- and disaccharides labelled with 2'GITag, 3'GITag and 4'GITag were isolated and characterised (see ESI section 1 of Fig. S1 and section 4 of Fig. S18-S23).

2.5. Optimisation of the *N*-glycan labelling procedure

Optimisation of derivatisation conditions, including adjustments to the temperature, duration, and solvent used for the derivatisation process, utilised *N*-glycans sourced from HRP. Throughout this optimisation phase, a single-variable approach was employed, while keeping constancy to all other variables. Following the optimisation of labelling conditions, the procedure involved adding a 20 µL aliquot of 2'GITag, 3'GITag or 4'GITag derivatisation solution (35 mM, containing 0.1 M sodium cyanoborohydride) to the *N*-glycan released from mouse serum samples. Each sample was vigorously vortexed until fully dissolved. They were then subjected to the optimised labelling conditions, which utilised 20 µL MeOH/acetic acid (7/3, v/v) as the solvent and were incubated at 65 °C for 2 h.

2.6. UPLC-ESI-MS analysis

The chromatographic and MS analysis of derivatized oligosaccharides and *N*-glycans was performed utilizing a Shimadzu LCMS 8040 system (Shimadzu Corporation, Kyoto, Japan), equipped with an LC-30 CE pump, a low-pressure gradient mixing unit, a SIL-30 AC autosampler and an electro spray ionisation (ESI) triple quadrupole system.

For the detection of oligosaccharides, the chromatographic separation was conducted using a reverse-phase C18 Hyperclone ODS 120 Å HPLC column (250 × 4.60 mm, 5 µm, Phenomenex, USA) with a flow rate of 0.8 mL/min at room temperature. The analysis was achieved with a binary solvent system consisting of NH₄HCO₃ (50 mM, pH 4.5) as solvent A and pure acetonitrile as solvent B. The gradient program began with 12–20 % solvent B from 0 to 3 min, then increased to 95 % in the next minute and held for an additional 2 min. Solvent B was subsequently reduced to 12 % within a minute, followed by an equilibration period under the same conditions for 3 min (ESI of section 1, Table S2).

The analysis of *N*-glycans labelled with GITags and 2AB underwent hydrophilic interaction liquid chromatography (HILIC) separation using a BEH Glycan column (1.7 µm, 2.1 × 150 mm, Waters) with a flow rate of 0.5 mL/min at 60 °C. The solvent system employed NH₄HCO₃ (50 mM, pH 4.5) as solvent A and acetonitrile as solvent B. The applied solvent gradient began with 95–78 % of solvent B over the initial 6 min, then decreased to 55.9 % over the next 44.5 min. Subsequently, solvent B was further decreased to 0 % within 1 min and held for 2 min before restoring to 95 % of solvent B, followed by a 3-minute equilibration period under the starting conditions (ESI of section 1, Table S3). The *N*-glycans were identified based on the combination of HPLC analysis, which provided preliminary information about glycan types through retention times and glucose unit (GU) values, and comparison with GU values of glycans in GlycoBase. The structures were then confirmed through analysis of mass-to-ratio (*m/z*) by ESI-MS in single ion monitoring (SIM) mode. *N*-glycans labelled with GITags can be monitored by LCMS in SIM mode, detecting ions including [M]⁺, [M + H]²⁺, and [M + Na]²⁺. The specific ions of glycans labelled with GITags are listed in ESI section 2, Tables S6-S8. The LCMS detection settings are provided in the ESI (Section 1, Table S4).

2.7. Statistical analysis

Each experiment was performed in triplicate. Results are expressed as mean ± standard deviation. Variance of analysis was performed using SPSS 21.0 software (IBM, Chicago, IL, USA). Different lowercase letters denote significant differences, which were assessed using Duncan's multiple range test (*p* < 0.01).

3. Results and discussion

3.1. Synthesis and characterisation of GITags (3–5)

The synthesis of the imidazolium-based MS reporter tag was pre-prepared

from 3-bromopropylamine hydrobromide **6** (Scheme 1A). Initially, the amine group in **6** was Boc-protected using Boc_2O and trimethylamine (TEA), resulting in bromide **7**. Subsequent reaction with 1-methylimidazolium to displace the bromide gave imidazolium **8** with a satisfactory 77 % yield across two steps. Next, Boc-deprotection with TFA exposed the amine group of **8**, leading to **9** in quantitative yield. To synthesize the variants 2'GITag (**3**), 3'GITag (**4**), and 4'GITag (**5**), a common approach was adopted, starting with aryl amino acids **10** (ortho), **15** (meta), and **20** (para). Amine Boc-protection as before led to intermediates **11**, **16**, and **21** in 45–70 % yields. Activation of the acidic moieties as *N*-hydroxysuccinimide (NHS)-esters **12**, **17** and **22** using 1-ethyl-3-(3-dimethylaminopropyl)carbodiimide hydrochloride (EDC-HCl) as condensing agent, and subsequent amide coupling with **9** provided the protected GITags **13**, **18**, and **23** with 10–35 % yields. The synthesis was completed by *N*-Boc deprotection under acidic conditions to yield 2'GITag (**3**), 3'GITag (**4**), and 4'GITag (**5**) in quantitative yields (For full details on synthetic procedures see ESI section 1).

3.2. Optimisation of labelling process

To optimise the glycan-derivatisation conditions of the new ITags in biological samples, the HRP glycoprotein was selected as a model source of *N*-glycans. The derivatisation process included an initial enzymatic glycan release through the use of PNGase (details in ESI, section 1) (Du et al., 2018). This was succeeded by the labelling procedure via non-reversible reductive amination (Fig. 2A). Parameters such as reaction time, temperature, and solvent choice were systematically adjusted to identify the optimal labelling conditions. The peak area of the predominant *N*-glycan compound (MMXF) was quantified and used as key parameter to evaluate the derivatisation efficiency through chromatographic analysis (Fig. 2B). The data revealed that increasing labelling time gave increased yields of labelled *N*-glycans peaking at 2 h. Further extension of the labelling time resulted in a reduction of the peak area of the MMXF *N*-glycan, likely due to the degradation of the labelled products over time (Fig. 2C). Therefore, the labelling duration of 2 h was determined to be optimal for subsequent experiments.

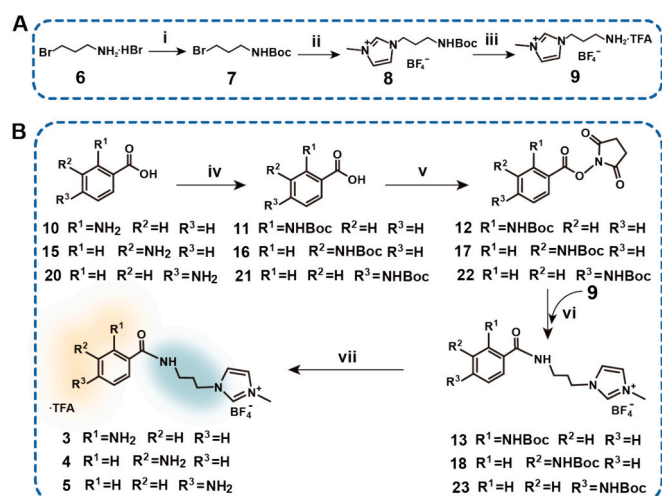
The screening of different reaction solvents including H_2O , DMSO, MeOH, EtOH and ACN in combination with acetic acid (7/3, v/v) was

also performed. Among those, the MeOH/acetic acid mixture exhibited the best derivatisation efficiency (Fig. 2D). Additionally, we investigated the influence of the reaction temperature on the yield of *N*-glycan derivatisation. The results showed that as the reaction temperature was gradually increased from 45 to 95 °C, the peak area of the MMXF *N*-glycan reached its maximum at 65 °C. Beyond this temperature, a decline in peak area was noted, which could be caused by the degradation of the reactants (Fig. 2E). Therefore, 65 °C was identified as the optimal reaction temperature for the following studies.

3.3. Quantitative analysis of derivatized oligosaccharides

In addressing the detection of oligosaccharides, our primary aim was not only to assess the fluorescence intensity and ionisation efficiency of our novel GITags compared to 2AB and our previously synthesized imidazolium-based tagging agent but also to ensure a comprehensive quantitative and qualitative analysis of derivatized oligosaccharides. For this purpose, GlcNAc and lactose were selected for a detailed analysis involving their limits of detection (LOD) and quantification (LOQ) using UPLC-ESI-MS. Hence, conjugates of *N*-acetylglucosamine (GlcNAc) and lactose (Lac) with 2'GITag (**3**), 3'GITag (**4**) and 4'GITag (**5**) were prepared and isolated on a preparative scale. The high polarity of both the GITags (**3–5**) and the corresponding ITagged-labelled GlcNAc and lactose products proved to be difficult to separate via silica gel chromatography. Therefore, to facilitate the purification of the GlcNAc and lactose GITag products, a 3-fold excess of GlcNAc or lactose over the targeted GITag and a 16-h reaction time were employed to ensure complete conversion of compounds (**3–5**) to the corresponding labelled glycosides. In this manner, the purification of the desired ITagged products over unlabeled glycosidic reagents through silica gel column chromatography was easily achieved. The labelled glycan-derivatives were successfully obtained with good yields, ranging from 74 % to 89 % (see ESI section 1 of Fig. S1). Serial dilutions of these oligosaccharides were prepared and subjected to UPLC-ESI-MS analysis. Given the specific *m/z* values for the GITags-conjugated oligosaccharides (GITags-GlcNAc, *m/z* 464, $[\text{M}]^+$; GITags-lactose, *m/z* 585, $[\text{M}]^+$), it was deemed unnecessary to collect each peak in separate vials for the purpose of comparing ionisation efficiencies and fluorescence intensities. Achieving distinct separation facilitates a direct and visual comparison of chromatograms obtained using different labels. This aspect not only enriches the quantitative analysis but also enables qualitatively assessing the efficacy of the GI-Tag by visually inspecting the chromatographic outputs. Furthermore, evaluations of the LOD and LOQ in terms of the fluorescence intensities and ionisation efficiencies of these compounds were performed as described in section 1 of the ESI (Fig. S4 and S5), with the results summarized in Table 1.

All the GITag derivatives provided LCMS LOD and LOQ values in the low fmol and sub-fmol range, outperforming the 2AB-labelled analogues in this aspect. Nonetheless, the fluorescence LOD and LOQ values were slightly higher than those of the 2AB-labelled counterparts. Remarkably, the 4'GITag labelled GlcNAc achieved an LOD of 1.2 fmol and an LOQ of 11.6 fmol, aligning with the values measured for the parent GITag (**2**). Moreover, the LOD of 4'GITag-labelled lactose was significantly enhanced, reaching the sub-fmol range (0.35 fmol), which underscores its exceptional sensitivity as a probe for LCMS glycan detection. This remarkable sensitivity enhancement suggests that the structural variations of the GITags have bolstered their MS sensitivity, with ionisation efficiencies far superior to those observed with 2AB-labelled oligosaccharides. The 4'GITag in particular, with its low LOD and LOQ, represents a valuable tool for the highly sensitive analysis of trace analytes in complex biological matrices. Such attributes designate the 4'GITag as an ideal probe for examining *N*-glycan biomarkers present on serum glycoproteins, facilitating their identification and understanding their implication in physiology and disease.



Scheme 1. Synthetic steps to access 4'GITag (**5**), 3'GITag (**4**) and 2'GITag (**3**). (A) Synthetic route of the imidazolium ionic liquid **9**. (B) Synthetic route of aromatic moiety and final GITag products. i) Boc_2O , TEA, DCM/ CH_3CN , 16 h, r. t., 58 % yield. ii) 1-methylimidazole, KBF_4 , CH_3CN , 16 h, reflux, 77 % yield. iii) TFA/DCM, 2 h, r. t., quant., 94 % yield. iv) Boc_2O , NaOH, THF/ H_2O , 16 h, r. t., 45–70 % yield. v) EDC-HCl, NHS, dry DMF, 16 h, r. t., 40–65 % yield. vi) Compound **9**, dry DMF, DIPEA, 6 h, 35 °C, 10–35 % yield. vii) DCM/TFA, 2 h, r. t., 85–95 % yield.

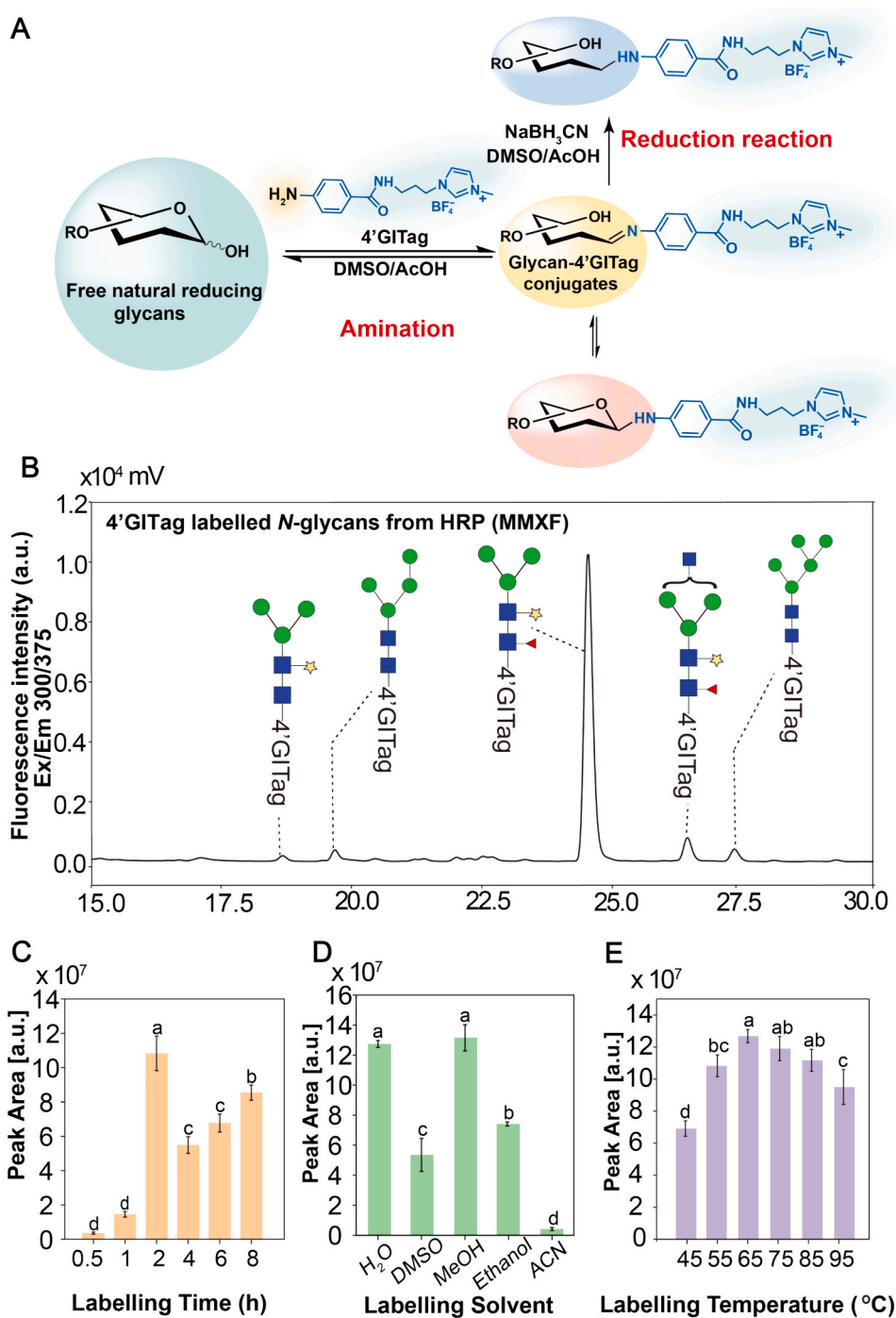


Fig. 2. General glycan derivatisation using the GITags (A). UPLC profile of 4'GITag labelled *N*-glycans from HRP (B). Labelling optimization study: Effect of different labelling times (C), different labelling solvents (D), and different labelling temperatures (E). All measurements were performed in triplicates. Different lowercase letters denote significant differences, which were assessed using Duncan's multiple range test ($p < 0.01$).

3.4. *N*-glycan profiling of mouse serum

To evaluate and benchmark the performance of 2'GITag (3), 3'GITag (4), and 4'GITag (5) in the derivatisation and subsequent detection of *N*-glycans from biological samples, mouse serum was chosen as model material. Each sample of mouse serum *N*-glycans was derivatized with the three different GITags and analysed using fluorescence detection. The findings indicated that samples derivatized with 4'GITag (5) exhibited the best fluorescence intensity and ionisation efficiency when compared to 2AB and the other GITag derivatives (Fig. 3). We also compared both the fluorescent HPLC and MS detection properties of

4'GITag (5) with procainamide (Pro A), a glycan reporter that recently demonstrated superior detection and profiling efficiency than 2AB (Keser et al., 2018; Klapoetke et al., 2010; Kozak et al., 2015). In total, twenty-four prominent *N*-glycan signals were detected with 4'GI-Tagged, comprising nineteen complex-type and five oligomannose-type *N*-glycans (Fig. 3A and B). The 4'GITag (5) outperformed the 2AB (1), 2'GITag (3), 3'GITag (4) and Pro A in terms of *N*-glycans detection efficiency. Specifically, with the 2AB standard, only six complex-type *N*-glycan species could be identified (Fig. 4C). For 2'GITag (3), seventeen *N*-glycan species were identified, including thirteen complex-types and four oligomannose-types. Meanwhile, 3'GITag (4), facilitated the

Table 1
LOD and LOQ of carbohydrates labelled by the four labels.

Compound	Fluorescence ^a		ESI-MS	
	LOD (fmol)	LOQ (fmol)	LOD (fmol)	LOQ (fmol)
2AB-GlcNAc ^b	58	189	476	731
4'GITag-GlcNAc	97	290	1.2	11.6
3'GITag-GlcNAc	1134	6967	17.8	33.7
2'GITag-GlcNAc	152	612	1.4	7.4
GITag-GlcNAc ^b	229	880	0.7	3.5
2AB-Lactose ^b	3.7	20	1080	2228
4'GITag-Lactose	241	792	0.35	6.76
3'GITag-Lactose	1001	3594	20	25
2'GITag-Lactose	142	554	7	13
GITag-Lactose ^b	211	602	3.1	9.7

^a Fluorescence intensities were measured at their maximum Ex/Em wavelengths (see ESI section 1 of Fig. S2).

^b Data compiled from reference (Zhang et al., 2021).

detection of fifteen *N*-glycan species, comprising eleven complex-type species and 4 oligomannose-type species (see Table S6-S8 in ESI of section 2). Although using Pro A as the fluorescent tag exhibited improved efficiency when compared to 2AB, only twenty-one *N*-glycan species were identified, including sixteen complex-types and five oligomannose-types (Fig. 5 and ESI section 2 Table S9). Compared to the conventional 2AB and Pro A labelling, 4'GITag (5) exhibited better

performance in the derivatisation and sensitive analysis of *N*-glycans, thereby underscoring the outstanding labelling efficiency of 4'GITag (5) for the detection and profiling of *N*-glycans in complex biological matrices.

Fifteen *N*-glycan species were consistently detected among the three GITag derivatisations, with relative abundances and profiles analysed through fluorescence UPLC and LCMS (Fig. 4A and B). Notably, two neutral *N*-glycans, FA2G1 and FA2, were the most abundant in mouse serum, correlating with the calculated $[M]^+$ and $[M + H]^2+$ ionic species (i.e. *N*-glycan FA2G1, $m/z = 1867.8$ and 933.9) after GITag derivatisation in LCMS (see ESI of section 2 Table S6). Six types of sialylated *N*-glycans, namely A3G3S3, A3G3S2, A3G3S, A2G2S2, FA2G2S2, and A2G2S, were successfully identified using all three GITags in the positive ion LCMS (see m/z and structures in ESI section 2 of Table S6-S8). The abundance of sialylated *N*-glycans labelled with 4'GITag (5) was higher than that labelled with 2'GITag (3) and 3'GITag (4), demonstrating the high sensitivity of 4'GITag (5), for sialylated *N*-glycans detection. Notably, samples labelled with GITags showed the A3G3S3 sialoglycan through both fluorescence and MS detection modes, whereas no LCMS signal for the 2AB-labelled A3G3S3 *N*-glycan was detected. This glycan has been recently recognized as a vital biomarker for predicting HIV rebound, thus indicating a lower likelihood of viral remission after antiretroviral therapy in patient sera. The abilities of the GITags, particularly the 4'GITag (5), to identify such intricate sialylation patterns and glycan biomarkers affirm their outstanding utility in glycomics research, offering significant implications for disease characterisation and

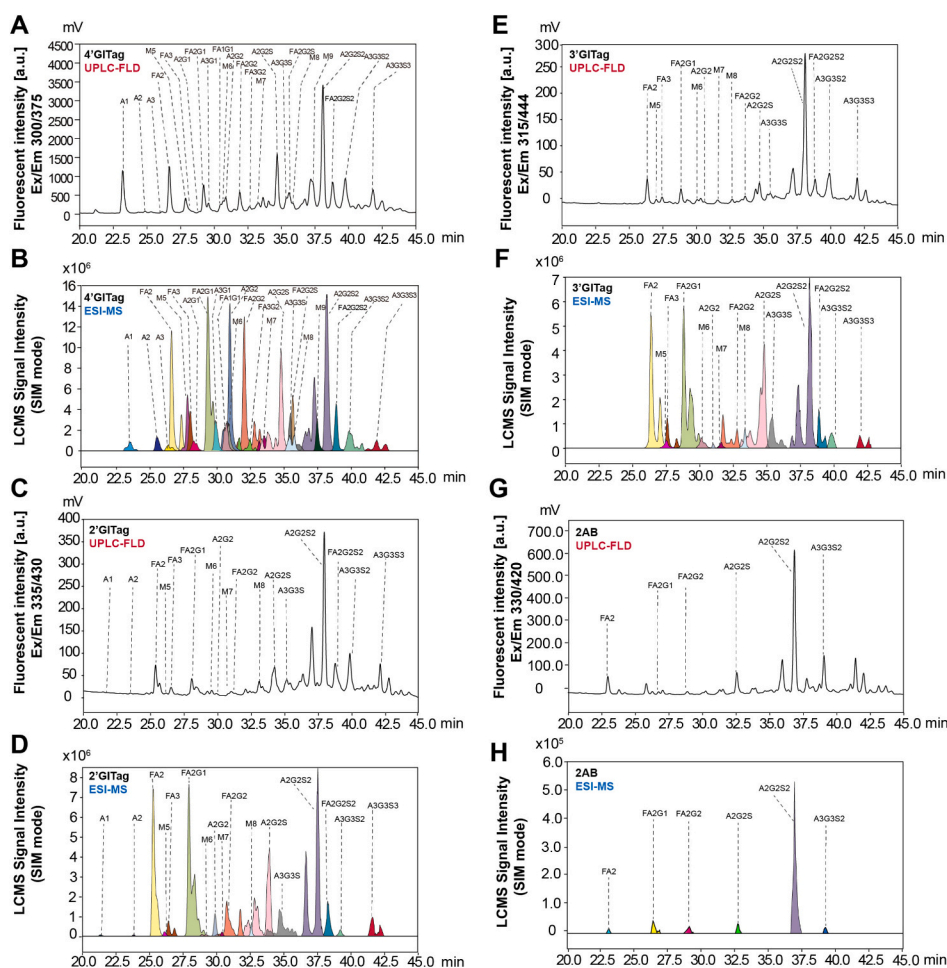


Fig. 3. LCMS and UPLC-fluorescence (FLD) profiles of mouse serum *N*-glycans labelled with four derivatisation reagents. (A) profile following 4'GITag labelling, (B) ESI-MS profile for 4'GITag-labelled *N*-glycans, leading into similar comparative profiles with (C) UPLC-FLD and (D) ESI-MS for 2'GITag, (E) UPLC-FLD and (F) ESI-MS for 3'GITag labelled specimens, and concluding with (G) UPLC-FLD and (H) ESI-MS profiles for 2AB-labelled *N*-glycans. A stands for GlcNAc, M for Mannose, F for Fucose, G for Galactose, S for Neu5Gc.

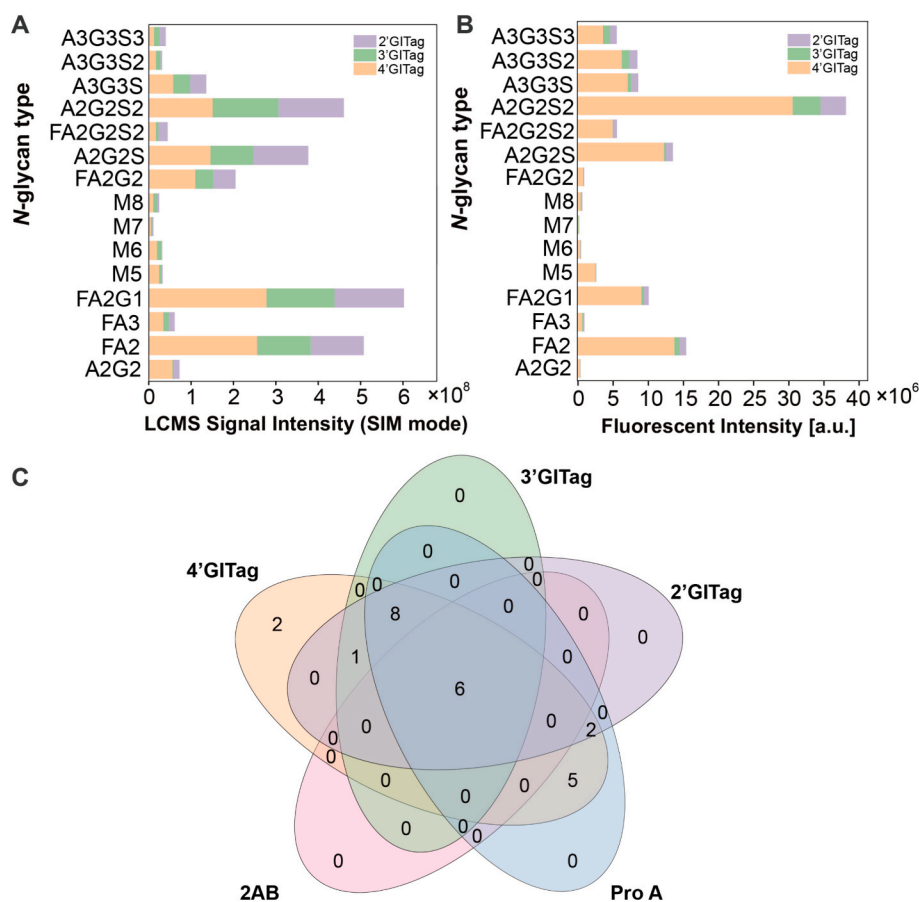


Fig. 4. Comparative analysis of *N*-glycans from mouse serum labelled with GITags. (A) LCMS signal intensity of the *N*-glycans from mouse serum labelled with 2'GITag, 3'GITag and 4'GITag. (B) Fluorescence signal intensity of the *N*-glycans from mouse serum labelled with 2'GITag, 3'GITag and 4'GITag. (C) Venn diagram showing the common and unique *N*-glycans labelled with five different derivatisation reagents.

biomarker discovery.

To further demonstrate the utility of 4'GITag (5) in the *N*-glycan profiling from plant biological samples, *N*-glycans from wasabi, mustard seeds, *Pleurotus eryngii*, and asparagus were extracted and derivatized with 4'GITag (5) and Pro A, respectively, then subjected to UPLC-ESI-MS detection. The results showed that 4'GITag (5), performed better than Pro A, facilitating the sensitive detection of plant-derived *N*-glycans (see ESI section 3 Fig. S7-S14). A total of 9 *N*-glycan species (5 oligomannose-type and 4 complex-type) could be observed in wasabi, 9 species (5 oligomannose-type and 4 complex-type) in mustard seeds, 5 species (5 oligomannose-type) in *Pleurotus eryngii*, and 10 species (1 oligomannose-type, and 9 complex-type) were detected in asparagus extracts (see ESI section 3 Table S10 and S11). The outstanding performance of 4'GITag (5) demonstrated the GITags' versatility as potent reporters facilitating the *N*-glycan detection and profiling across different biological samples. This feature could be employed in novel biomedical applications, such as in the exploration of the relationship between dietary *N*-glycans and allergic reactions.

4. Conclusion

We report the synthesis of three novel imidazolium ionic derivatisation reagents (2'GITag (3), 3'GITag (4), 4'GITag (5)) and demonstrate their use as sensitive tools for glycan analysis. Among them, the 4'GITag (5) exhibited the best fluorescence and MS detection, making it an outstanding glycan labelling reagent. Notably, it enabled the detection of model oligosaccharides down to the sub-fmol region, showing significantly superior LOD and LOQ values than the standard 2AB reporter. Optimal labelling of *N*-glycans was achieved in MeOH/acetic

acid (7/3, v/v) at 65 °C for 2 h. The novel GITags facilitated the sensitive detection of glycans in biological matrices, with 4'GITag (5) enabling the identification of 24 distinct *N*-glycans in mouse serum, including A3G3S3, a critical biomarker for the study of HIV antiretroviral therapeutic efficacy; in contrast, only 6 *N*-glycans were detected using 2AB-labelling and 21 *N*-glycans were detected using Pro A labelling. It is noteworthy that the sensitivity of *N*-glycans labelled with 4'GITag (5) in fluorescence and mass spectrometry detection surpasses that of Pro A, which is known for its high detection sensitivity, further highlighting the superior performance of 4'GITag (5) in glycan analysis from complex biological samples. Therefore, the combination of 4'GITag (5) and high-end mass spectrometry will provide a promising platform for glycan analysis at the glycomics level. Further applications for glycan derivatisation of tissue and plant samples are anticipated, allowing the exploration and detection of biologically relevant biomarkers for early diagnosis, the study of disease progression, and relationship between dietary *N*-glycans and allergic reactions.

CRedit authorship contribution statement

Yao-Yao Zhang: Writing – review & editing, Writing – original draft, Methodology, Investigation, Formal analysis, Data curation. **Si-Yu Zhang:** Writing – review & editing, Methodology, Investigation, Formal analysis, Data curation. **Zi-Xuan Hu:** Writing – review & editing, Methodology, Investigation, Formal analysis, Data curation. **Josef Voglmeir:** Writing – review & editing, Writing – original draft, Validation, Supervision, Project administration, Funding acquisition, Formal analysis, Conceptualization. **Li Liu:** Writing – review & editing, Writing – original draft, Validation, Project administration,

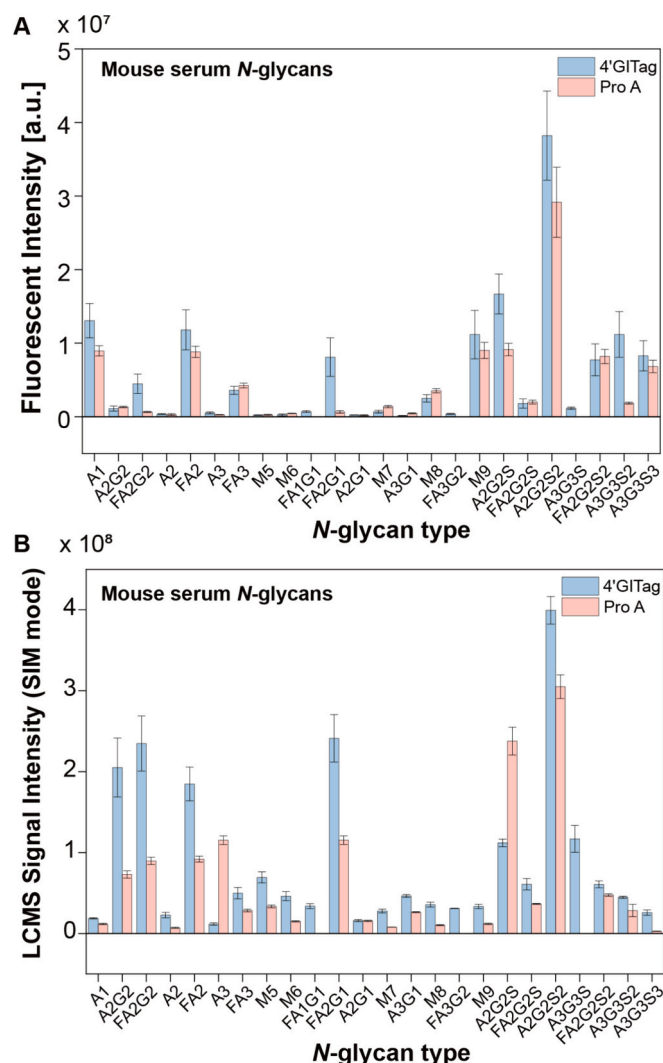


Fig. 5. Comparative analysis of *N*-glycans from mouse serum labelled with GITags. (A) Fluorescence signal intensity of the *N*-glycans from mouse serum labelled with 4'GITag and Pro A. (B) LCMS signal intensity of the *N*-glycans from mouse serum labelled with 4'GITag and Pro A.

Investigation, Funding acquisition, Formal analysis. **M. Carmen Galan:** Writing – review & editing, Writing – original draft, Validation, Supervision, Funding acquisition, Formal analysis, Data curation, Conceptualization. **Mattia Ghirardello:** Writing – review & editing, Writing – original draft, Supervision, Investigation, Formal analysis, Data curation, Conceptualization.

Declaration of competing interest

The authors declare that they have no known competing financial interests or personal relationships that could have appeared to influence the work reported in this paper.

Data availability

Data will be made available on request.

Acknowledgements

This work was supported by the EPSRC GCRFE (Grant Nos. P/T020288/1 and EP/S026215/1 (to MCG and MG)), ERC COG (Grant Nos 648239 (MCG)), National Natural Science Foundation of China (Grant

Nos. 31471703, 31671854, 31871793 and 31871754 (to JV and LL)). MG acknowledges the European Union's Horizon 2020 research and innovation programme under the Marie Skłodowska-Curie grant agreement No 101034288 for financial support.

Appendix A. Supplementary data

Supplementary data to this article can be found online at <https://doi.org/10.1016/j.carbpol.2024.122449>.

References

- Aich, U., Hurum, D. C., Basumallick, L., Rao, S., Pohl, C., Rohrer, J. S., & Kandzia, S. (2014). Evaluation of desialylation during 2-amino benzamide labeling of asparagine-linked oligosaccharides. *Analytical Biochemistry*, *458*, 27–36.
- Alagesan, K., Hinneburg, H., Seeberger, P. H., Silva, D. V., & Kolarich, D. (2019). Glycan size and attachment site location affect electron transfer dissociation (ETD) fragmentation and automated glycopeptide identification. *Glycoconjugate Journal*, *36* (6), 487–493.
- Alvarez, M. R. S., Zhou, Q., Tena, J., Lebrilla, C. B., Completo, G. C., Heralde, F. M. I., ... Nacario, R. C. (2022). *N*-glycan and glycopeptide serum biomarkers in philippine lung cancer patients identified using liquid chromatography–Tandem mass spectrometry. *ACS Omega*, *7*(44), 40230–40240.
- Bechtella, L., Chunsheng, J., Fentker, K., Ertürk, G. R., Saffertal, M., Polewski, A., ... Pagel, K. (2024). Ion mobility-tandem mass spectrometry of mucin-type *O*-glycans. *Nature Communications*, *15*(1), 2611.
- Benito-Alifonso, D., Tremell, S., Sadler, J. C., Berry, M., & Galan, M. C. (2016). Imidazolium-tagged glycan probes for non-covalent labeling of live cells. *Chemical Communications*, *52*(27), 4906–4909.
- Bones, J., Mittermayr, S., O'Donoghue, N., Guttman, A., & Rudd, P. M. (2010). Ultra performance liquid chromatographic profiling of serum *N*-glycans for fast and efficient identification of cancer associated alterations in glycosylation. *Analytical Chemistry*, *82*(24), 10208–10215.
- Cai, Z. P., Hagan, A. K., Wang, M. M., Flitsch, S. L., Liu, L., & Voglmeir, J. (2014). 2-Pyridylfuran: A new fluorescent tag for the analysis of carbohydrates. *Analytical Chemistry*, *86*(10), 5179–5186.
- Cai, Z. P., Wang, W. L., Conway, L., Huang, K., Awad, F. N., Liu, L., & Voglmeir, J. (2017). 1, 3-Di(2-dipyrlyl)propan-1, 3-dione – A new fluorogenic labeling reagent for milk oligosaccharides. *Pure & Applied Chemistry*, *89*(7), 921–929.
- Cho, B. G., Gutierrez, R. C., Goli, M., Gautam, S., Banazadeh, A., & Mechref, Y. (2022). Targeted *N*-Glycan analysis with parallel reaction monitoring using a quadrupole-orbitrap hybrid mass spectrometer. *Analytical Chemistry*, *94*(44), 15215–15222.
- Du, Y. M., Zheng, S. L., Liu, L., Voglmeir, J., & Yedig, G. (2018). Analysis of *N*-glycans from *Raphanus sativus* cultivars using PNGase H⁺. *Jove-Journal of Visualized Experiments*, *25*(136), 57979.
- Ghirardello, M., Zhang, Y. Y., Voglmeir, J., & Galan, M. C. (2022). Recent applications of ionic liquid-based tags in glycoscience. *Carbohydrate Research*, *520*, Article 108643.
- Giron, L. B., Palmer, C. S., Liu, Q., Yin, X., Papisavvas, E., Sharaf, R., ... Abdel-Mohsen, M. (2021). Non-invasive plasma glycomic and metabolic biomarkers of post-treatment control of HIV. *Nature Communications*, *12*(1), 3922.
- Guo, R. R., Comamala, G., Yang, H. H., Gramlich, M., Du, Y. M., Wang, T., ... Voglmeir, J. (2020). Discovery of highly active recombinant PNGase H⁺ variants through the rational exploration of unstudied acidobacterial genomes. *Frontiers in Bioengineering and Biotechnology*, *8*, 741.
- Keser, T., Pavić, T., Lauc, G., & Gornik, O. (2018). Comparison of 2-aminobenzamide, procainamide and rapifluor-MS as derivatizing agents for high-throughput HILIC-UPLC-FLR-MS *N*-glycan analysis. *Frontiers in Chemistry*, *6*, 324.
- Kianfar, E. (2020). Ionic liquids: Properties, application, and synthesis. *Fine Chemical Engineering*, *2*, 22–31.
- Kizuka, Y., Kitazume, S., & Taniguchi, N. (2017). *N*-glycan and Alzheimer's disease. *Biochimica et Biophysica Acta-General Subjects*, *1861*(10), 2447–2454.
- Klapoetke, S., Zhang, J., Becht, S., Gu, X., & Ding, X. (2010). The evaluation of a novel approach for the profiling and identification of *N*-linked glycan with a procainamide tag by HPLC with fluorescent and mass spectrometric detection. *Journal of Pharmaceutical and Biomedical Analysis*, *53*(3), 315–324.
- Kozak, R. P., Tortosa, C. B., Fernandes, D. L., & Spencer, D. I. (2015). Comparison of procainamide and 2-aminobenzamide labeling for profiling and identification of glycans by liquid chromatography with fluorescence detection coupled to electrospray ionization-mass spectrometry. *Analytical Biochemistry*, *486*, 38–40.
- Le, H. T., Park, K. H., Jung, W., Park, H. S., & Kim, T. W. (2018). Combination of microwave-assisted girard derivatization with ionic liquid matrix for sensitive MALDI-TOF MS analysis of human serum *N*-Glycans. *Journal of Analytical Methods in Chemistry*, *2018*, 1–7.
- Li, Z., Wang, X., Deng, X., Song, J., Yang, T., Liao, Y., Gong, G., Huang, L., Lu, Y., & Wang, Z. (2023). High-sensitivity qualitative and quantitative analysis of human, bovine and goat milk glycosphingolipids using HILIC-MS/MS with internal standards. *Carbohydrate Polymers*, *312*, Article 120795.
- Liu, Y., Hu, X., Voglmeir, J., & Liu, L. (2023). *N*-glycan profiles as a tool in qualitative and quantitative analysis of goat milk adulteration. *Food Chemistry*, *423*, Article 136116.

- Luo, G., Jin, K., Deng, S., Cheng, H., Fan, Z., Gong, Y., Qian, Y., Huang, Q., Ni, Q., Liu, C., & Yu, X. (2021). Roles of CA19-9 in pancreatic cancer: Biomarker, predictor and promoter. *Biochimica Et Biophysica Acta-Reviews on Cancer*, 1875(2), Article 188409.
- Magalhães, A., Duarte, H. O., & Reis, C. A. (2017). Aberrant glycosylation in cancer: A novel molecular mechanism controlling metastasis. *Cancer Cell*, 31(6), 733–735.
- Mahmoudi, H., Valentini, F., Ferlin, F., Bivona, L. A., Anastasiou, I., Fusaro, L., ... Vaccaro, L. (2019). A tailored polymeric cationic tag–anionic Pd(ii) complex as a catalyst for the low-leaching Heck–Mizoroki coupling in flow and in biomass-derived GVL. *Green Chemistry*, 21(2), 355–360.
- Malaker, S. A., Riley, N. M., Shon, D. J., Pedram, K., Krishnan, V., Dorigo, O., & Bertozzi, C. R. (2022). Revealing the human mucinome. *Nature Communications*, 13(1), 3542.
- Manz, C., Mancera-Arteu, M., Zappe, A., Hanozin, E., Polewski, L., Giménez, E., ... Pagel, K. (2022). Determination of sialic acid isomers from released N-Glycans using ion mobility spectrometry. *Analytical Chemistry*, 94(39), 13323–13331.
- Marie, A. L., Ray, S., & Ivanov, A. R. (2023). Highly-sensitive label-free deep profiling of N-glycans released from biomedically-relevant samples. *Nature Communications*, 14(1), 1618.
- Melo, D. J., Moran, A. B., Peel, S. R., Hendel, J. L., & Spencer, D. (2022). Egg yolk sialylglycopeptide: Purification, isolation and characterization of N-glycans from minor glycopeptide species. *Organic & Biomolecular Chemistry*, 20(24), 4905–4914.
- Mereiter, S., Balmaña, M., Campos, D., Gomes, J., & Reis, C. A. (2019). Glycosylation in the era of cancer-targeted therapy: Where are we heading? *Cancer Cell*, 36(1), 6–16.
- Messina, A., Palmigiano, A., Esposito, F., Fiumara, A., Bordugo, A., Barone, R., Sturiale, L., Jaeken, J., & Garozzo, D. (2021). HILIC-UPLC-MS for high throughput and isomeric N-glycan separation and characterization in Congenital Disorders Glycosylation and human diseases. *Glycoconjugate Journal*, 38(2), 201–211.
- Pallister, E. G., Choo, M., Walsh, I., Tai, J. N., Tay, S. J., Yang, Y. S., ... Nguyen-Khuong, T. (2020). Utility of ion-mobility spectrometry for deducing branching of multiply charged glycans and glycopeptides in a high-throughput positive ion LC-FLR-IMS-MS workflow. *Analytical Chemistry*, 92(23), 15323–15335.
- Quintana, J. I., Atxabal, U., Unione, L., Ardá, A., & Jiménez-Barbero, J. (2023). Exploring multivalent carbohydrate-protein interactions by NMR. *Chemical Society Reviews*, 52(5), 1591–1613.
- Reily, C., Stewart, T. J., Renfrow, M. B., & Novak, J. (2019). Glycosylation in health and disease. *Nature Reviews Nephrology*, 15(6), 346–366.
- Ressom, H. W., Varghese, R. S., Goldman, L., Loffredo, C. A., Abdel-Hamid, M., Kyselova, Z., ... Goldman, R. (2008). Analysis of MALDI-TOF mass spectrometry data for detection of glycan biomarkers. *Pacific Symposium on Biocomputing*, 13, 216–227.
- Sasaki, G. L., Guerrini, M., Serrato, R. V., Santana, F. A., Carlotto, J., Simas-Tosin, F., ... Gorin, P. A. (2014). Monosaccharide composition of glycans based on Q-HSQC NMR. *Carbohydrate Polymers*, 104, 34–41.
- Schjoldager, K. T., Narimatsu, Y., Joshi, H. J., & Clausen, H. (2020). Global view of human protein glycosylation pathways and functions. *Nature Reviews. Molecular Cell Biology*, 21(12), 729–749.
- Sethi, M. K., Hancock, W. S., & Fanayan, S. (2016). Identifying N-Glycan biomarkers in colorectal cancer by mass spectrometry. *Accounts of Chemical Research*, 49(10), 2099–2106.
- Shao, N., Xue, J., & Guo, Z. (2003). Chemical synthesis of CD52 glycopeptides containing the acid-labile fucosyl linkage. *The Journal of Organic Chemistry*, 68(23), 9003–9011.
- Sittel, I., & Galan, M. C. (2015). Chemo-enzymatic synthesis of imidazolium-tagged sialyllactosamine probes. *Bioorganic & Medicinal Chemistry Letters*, 25(19), 4329–4332.
- Varki, A. (2017). Biological roles of glycans. *Glycobiology*, 27(1), 3–49.
- Vos, G. M., Hooijschuur, K. C., Li, Z., Fjeldsted, J., Klein, C., de Vries, R. P., ... Boons, G. (2023). Sialic acid O-acetylation patterns and glycosidic linkage type determination by ion mobility-mass spectrometry. *Nature Communications*, 14(1), 6795.
- Wagt, S., de Haan, N., Wang, W., Zhang, T., Wuhler, M., & Lageveen-Kammeijer, G. S. M. (2022). N-Glycan isomer differentiation by zero flow capillary electrophoresis coupled to mass spectrometry. *Analytical Chemistry*, 94(38), 12954–12959.
- Wright, J. N., Collins, H. E., Wende, A. R., & Chatham, J. C. (2017). O-GlcNAcylation and cardiovascular disease. *Biochemical Society Transactions*, 45(2), 545–553.
- Zhang, Y., Bu, R., Cao, Y., Jin, J., Meng, K., & Qiu, F. (2022). A rapid 2AB-UHPLC method based on magnetic beads extraction for N-glycan analysis of recombinant monoclonal antibody. *Journal of Chromatography B-Analytical Technologies in The Biomedical and Life Sciences*, 1192, Article 123139.
- Zhang, Y. Y., Ghirardello, M., Wang, T., Lu, A. M., Liu, L., Voglmeir, J., & Galan, M. C. (2021). Imidazolium labelling permits the sensitive mass-spectrometric detection of N-glycosides directly from serum. *Chemical Communications*, 57, 7003–7006.
- Zhang, Y. Y., Senan, A. M., Wang, T., Liu, L., & Voglmeir, J. (2019). 1-(2-Aminoethyl)-3-methyl-1H-imidazol-3-ium tetrafluoroborate: Synthesis and application in carbohydrate analysis. *Pure and Applied Chemistry*, 91, 1441–1450.
- Zhou, X., Song, W., Novotny, M. V., & Jacobson, S. C. (2022). Fractionation and characterization of sialyl linkage isomers of serum N-glycans by CE-MS. *Journal of Separation Science*, 45(17), 3348–3361.
- Zhu, J., Wu, J., Yin, H., Marrero, J., & Lubman, D. M. (2015). Mass spectrometric N-glycan analysis of haptoglobin from patient serum samples using a 96-well plate format. *Journal of Proteome Research*, 14(11), 4932–4939.
- Zilmer, M., Edmondson, A. C., Khetarpal, S. A., Alesi, V., Zaki, M. S., Rostasy, K., ... Møller, R. S. (2020). Novel congenital disorder of O-linked glycosylation caused by GALNT2 loss of function. *Brain: a Journal of Neurology*, 143(4), 1114–1126.